Analysis and Damping of Harmonic Propagation in DG-Penetrated Distribution Networks

Lu, Jinghang; Savaghebi, Mehdi; Guerrero, Josep M.

Analysis and Damping of Harmonic Propagation in DG-Penetrated Distribution Networks

Jinghang Lu, Mehdi Savaghebi, Josep M.Guerrero

Department of Energy Technology

Aalborg University, Denmark

{jgl,mes,joz}@et.aau.dk

Abstract—**With the increasing penetration of nonlinear loads into distribution system, stable operation of power distribution system suffers challenge by harmonic voltage propagation and resonance amplification which is also known as whack-a-mole phenomenon. However, until now this phenomenon has not been well investigated and discussed. This paper starts from theoretical analysis of harmonic propagation and how it is triggered when DG unit interfaced to the grid. Moreover, harmonic damping performance of various types of impedance seen from DG at selected frequencies are analyzed and compared by introducing microwave transmission line theory. In addition, this paper proposes a control algorithm with DG unit where virtual impedances at selected frequencies are individually designed to mitigate the harmonic amplification. The validity of the control strategy has been verified by the case study results.**

Keywords—*Power quality; resonance propagation; distributed generation; virtual impedance;*

I. INTRODUCTION

Last few years has witnessed the high penetration of nonlinear loads, such as rectifier diodes and switching power electronic devices into grid [1]. These nonlinear loads can result in significant harmonic pollution in the distribution networks, where harmonic propagation occurs and resonance amplifies along the line [2]. In order to mitigate the harmonic propagation and resonance amplification, installations of active and passive filter have been adopted in the long power distribution system. However, adoption of passive filter to damp the harmonic is fading out due to several reasons, such as power loss, bulky volume and additional cost [2]. On the other hand, resistive active power filter(R-APF) [3] is becoming a promising method as the flexible control strategies of R-APF are able to emulate the passive damping characteristic at the selected harmonic frequency [2]-[6]. However, It has been reported that installation of active power filter may cause the phenomenon of "whack-a-mole" [4]. This phenomenon is referred to as the harmonic that is mitigated by installation of R-APF in some nodes of the feeder amplifies on other nodes where no R-APF is installed. To solve this issue, literature [4] points out that R-APF which is installed at the end of the long distribution feeder can effectively damp out amplification of harmonics. In addition, in recent years several control methods of R-APF have been proposed to enhance its capability of mitigating harmonics, among which a discrete frequency-tuning active power filter [5] which operates as a variable conductance at the selected frequency is proposed

to suppress the grid harmonics. Meanwhile, [6] proposed a multiple R-APFs method, where harmonic sharing is achieved by tuning the droop control gain. Moreover, double R-APFs have been installed at different installation point along the distribution feeder to suppress the harmonics [7]. But this control method may be sensitive to the installation point, resulting in severe harmonic amplification.

On the other hand, nowadays, the concept of Renewable Energy Source(RES) based Distributed Generation(DG) units with the capability to address power quality issues has drawn much attention. By adding the R-APF function into current or voltage reference of grid-interfacing converter, power quality improvement can be achieved without affecting the primary control strategy. In [8], R-APF function has been incorporated into primary DG power control by carrying out current-controlled method(CCM). But CCM can hardly support voltage at Point of Common Coupling (PCC) when the DG unit intentionally works in islanding mode[9]. To improve the performance in grid-connecting mode, islanding mode as well as the transition between them, Voltage-Controlled Method (VCM) has been implemented in [10], where DG unit is controlled to be virtual impedance looking inside from LC filter. Combined with physical feeder impedance, VCM-virtual impedance strategy could improve power quality at PCC by sacrificing the power quality of capacitor voltage of output filter. Although the aforementioned works are able to address certain power quality problems, the "whack-a-mole" issue on a long distribution feeder has not been systematically analyzed.

To elaborately discuss harmonic propagation and amplification phenomenon, a detailed theoretical analysis based on the distributed parameter model [11] will be presented by introducing microwave transmission line theory. Characteristic of harmonic voltage propagation and resonance will be investigated when various types of impedance are connected at the terminal of the long feeder. Besides, an improved virtual impedance based active damping method of DG that consists of virtual resistor and virtual inductor at selected frequencies is implemented. This simple and effective method is able to eliminate the impact of grid-side inductor of DG meanwhile achieve optimal harmonic damping along the feeder.

II. MODELING OF POWER DISTRIBUTION FEEDER

Fig.1 shows a lumped-parameter model of distribution feeder while TABLE 1 provides the system parameter information. Besides, for sake of simplicity, it is assumed that feeder inductance, resistance and capacitance are evenly distributed in the feeder.
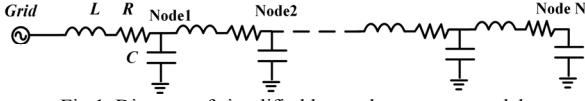

Fig.1. Diagram of simplified lumped parameter model

TABLE I.   DISTRIBUTED FEEDER PARAMETERS

	Value
Feeder length	10km
Line Inductance L	1.98 mH/km
Line Capacitance C	$25\mu F$/km
Parasite resistance R	0.12Ω/km

According to transmission line theory, the characteristic impedance Z_0' of a general feeder is given by:

$$Z_0' = \sqrt{\frac{R+jwL}{jwC}} \qquad (1)$$

Where R, L and C, as is shown in Fig.1, are feeder equivalent resistance, inductance and capacitance, w is the angular frequency. To analyze the harmonic propagation phenomenon, the worst case ($R = 0$) will be considered in the following analysis as the feeder resistance will provide inherent damping for the harmonic propagation. Therefore, by omitting inherent damping resistance (1) will be expressed as:

$$Z_0 = \sqrt{\frac{L}{C}} \qquad (2)$$

Moreover, the propagation constant γ and wavelength λ are expressed in (3) and (4), w_h is the harmonic voltage angular frequency[4].

$$\gamma = j\beta = jw_h\sqrt{LC} \qquad (3)$$
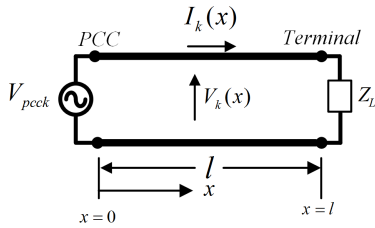
$$\lambda = \frac{2\pi}{w_h\sqrt{LC}} \qquad (4)$$

Fig.2.Diagram of single phase distributed-parameter model

In.Fig.2, the distributed model of long power distribution feeder is depicted considering this fact that the lumped parameter can not precisely illustrate the harmonic resonance propagation characteristic in such feeder. In this figurethe kth harmonic voltage at the PCC V_{pcck} is assumed to be stiff, terminal of the feeder is connected to the impedance Z_L. In order to make a general discussion, Z_L can be a real passive impedance or a virtual impedance at selected harmonic frequencies, since DG unit with virtual impedance embedded in the control loop can be modeled by an equivalent harmonic impedance at the end of the feeder. In addition, the length of the feeder is l. x is the distance from PCC.

From [1], harmonic voltage-current standing wave equations at the distance x is expressed as:

$$V_k(x) = A_1 e^{-j\beta x} + A_2 e^{j\beta x} \qquad (5)$$

$$I_k(x) = \frac{1}{Z_0}(A_1 e^{-j\beta x} - A_2 e^{j\beta x}) \qquad (6)$$

Where Z_0 is the characteristic impedance of the feeder shown in (2), A_1 and $A_2$are separately defined as the forward moving wave coefficient and backward moving wave coefficient which are determined by feeder's boundary condition. In this paper the following boundary conditions are satisfied:

$$V_k(0) = V_{pcck} \qquad (7)$$

$$\frac{V_k(l)}{I_k(l)} = Z_L \qquad (8)$$

Where Z_L represent general impedance that an be real passive impedance or virtual impedance .

Therefore, by solving (5),(6),(7),(8), The following equations are derived:

$$A_1 = \frac{(\cosh(rl)+\sinh(rl))(Z_L+Z_0)}{2(Z_L\cosh(rl)+Z_0\sinh(rl))}, \ A_2 = \frac{(\sinh(rl)-\cosh(rl))(Z_0-Z_L)}{2(Z_L\cosh(rl)+Z_0\sinh(rl))} \qquad (9)$$

Substituting A_1 and A_2 into (5) formulates the harmonic voltage expression at distance x:

$$V_k(x) = \frac{Z_L\cosh(r(l-x))+z\sinh(r(l-x))}{Z_L\cosh(rl)+z\sinh(rl)} \qquad (10)$$

However, in order to have a deep investigation of harmonic propagation characteristic which can be hardly observed from (10), the coordinate original point of Fig.2 will be set at the terminal and details will be discussed in the next section.

III. ANALYSIS OF VOLTAGE HARMONIC PPOPAGATION

In this section, virtual impedance of DG control strategy will be discussed first. Fig.3 illustrates the configuration of single
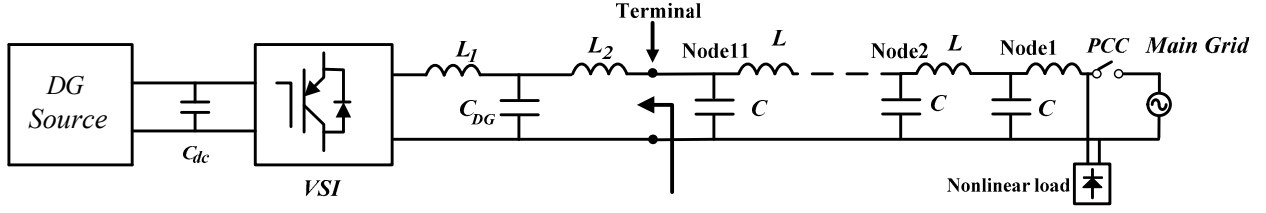
Fig.3.Configuration of single phase DG to the main grid through long power distribution feeder

phase DG system that connects to the power distribution networks at the terminal of the feeder. Besides, a nonlinear load is connected at PCC and the Static Transfer Switch (STS) is controlled on and off to switch the DG's operation from grid-connected mode to islanding mode

It has been demonstrated [8] that DG unit with CCM can incorporate virtual impedance in the control loop by adding a harmonic current reference to the fundamental current reference that is expressed as:

$$I_{ref} = I_{reff} - H_B \cdot \frac{V(l)}{R_v} \qquad (11)$$

Where I_{reff} is the fundamental current reference, $V(l)$ is the measured DG output voltage at the terminal, H_B is the bandpass filter at the selected frequency, R_v is the virtual resistance at the respective frequency. It is noteworthy that if virtual impedance from (11) is not embedded in the current reference generation which implies $R_v = \infty$ at the selected harmonic frequency, DG unit viewed from the terminal of the feeder is open-circuit at the selected frequency.

Alternatively, DG unit with VCM is able to integrate the virtual impedance term by adding a current feedforward term in the voltage reference which is described as:

$$V_{ref} = V_{reff} - R_v \cdot (H_B \cdot I_{DG}) \qquad (12)$$

Where V_{reff} is the fundamental voltage reference coming from droop control scheme, H_B is the bandpass filter at the selected frequency, R_v is the virtual impedance at the selected frequency seen inside DG from the terminal. Note that VCM based DG unit output filter is commonly selected to be LC or LCL filter, if the harmonic compensation $R_v \cdot (H_B \cdot I_{DG})$ is not included in (12), which implies $R_v = 0$, DG unit with LC filter will be viewed as short circuit from terminal at the respective frequency, alternatively, DG unit with LCL filter will be treated as pure inductance at the selected frequency.

Based on aforementioned discussion, Fig.4 illustrate the 3th, 5th,7th and 9th harmonic voltage amplification along the 10km feeder when the nonlinear load is connected to the PCC and terminal of feeder is either open-circuit, short-circuit or connected to pure inductance to emulate the CCM and VCM without harmonic compensation scenario. Take open circuit situation as an example where 7th harmonic voltage propagated along the feeder. (Fig.3(c)). It can be observed that 7th harmonic voltage greatly amplifies at 10 km whereas diminishes at around 6.8 km.

Meanwhile, in short circuit case, it is observed from Fig.3(b) and (d) that 5th and 9th harmonics are extremely amplified when terminal is short-circuit, while 3rd harmonic's maximum voltage

(a)

(b)

(c)

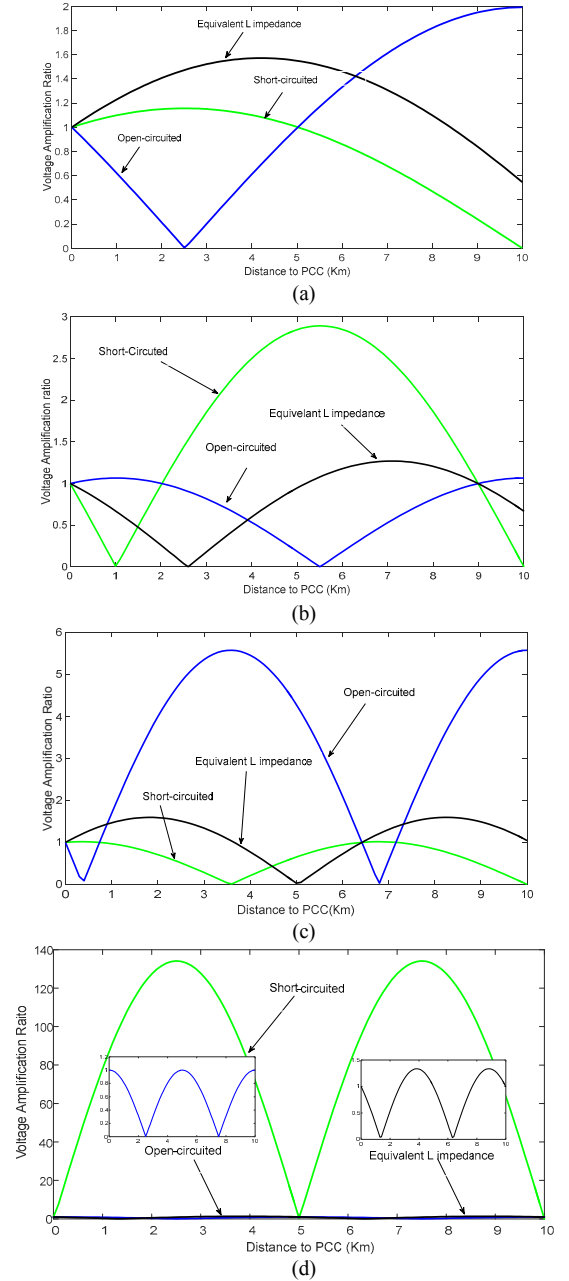
(d)

Fig.4. Harmonic voltage amplification ratio when 3th (a) 5[th](b), 7[th](c), 9th (d) harmonic voltage source is connected to the PCC

occurs at the terminal of the feeder. Moreover, if DG with LCL filter works at primary power injection mode by adopting VCM method, harmonic voltage will drop on the LCL grid side filter L_2[12], resulting in harmonic amplification along the feeder as

well. But the principle of how these harmonics are amplified and what affects the amplitude of harmonic propagation has not been deeply investigated. The following part of this section will discuss this issue.
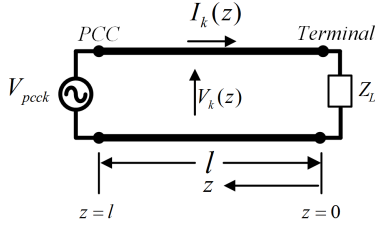

Fig.5.Diagram of single phase distributed-parameter model

From (9), it is observed that A_1 and A_2 are the wave coefficients that have no relationship with distance x. Therefore, if the Original point is set at the terminal as shown in Fig.5, substitute $z = -x$ into (5) and (6), voltage and current along the feeder can be expressed as:

$$V_k(z) = V_i(z) + V_r(z) = A_1 e^{j\beta z} + A_2 e^{-j\beta z} \quad (13)$$

$$I_k(z) = \frac{1}{Z_L}(A_1 e^{j\beta z} - A_2 e^{-j\beta z}) \quad (14)$$

Where $V_i(z)$ and $V_r(z)$ are defined as voltage forward travelling wave and backward travelling wave, which are expressed as:

$$V_i(z) = A_1 e^{j\beta z} \text{ and } V_r(z) = A_2 e^{-j\beta z} \quad (15)$$

Meanwhile, the reflection coefficient is defined as:

$$\Gamma = \frac{V_r(z)}{V_i(z)} = \frac{A_2 e^{-j\beta z}}{A_1 e^{j\beta z}} = \frac{A_2}{A_1} e^{-2j\beta z} \quad (16)$$

At the position of $z=0$, from (16) it can be found that

$$\Gamma_L = \frac{V_r(0)}{V_i(0)} = \frac{Z_L - Z_0}{Z_L + Z_0} \quad (17)$$

Where $V_i(0)$ and $V_r(0)$ are described as forward travelling wave and backward travelling wave at the position of $z=0$ (that is terminal of the feeder), In addition, Z_L and Z_0 are respectively the terminal impedance and characteristic impedance.

In the following part, various types of terminal impedance will be investigated.

A. Short-circuit case

The terminal is short-circuited ($Z_L = 0$), which implies voltage amplitude at the terminal is zero. Substituting $z = 0$ into (13) and (14) result in the following expression:

$$V_k(0) = A_1 + A_2 = V_{iL} + V_{rL} = 0 \Rightarrow V_{iL} = -V_{rL}, A_1 = -A_2 \quad (18)$$

$$I_k(0) = \frac{1}{Z_L}(A_1 - A_2) = I_{iL} + I_{rL}$$
$$= \frac{1}{Z_L}(V_{iL} - V_{rL}) = 2\frac{V_{iL}}{Z_L} = 2I_{iL} \Rightarrow I_{iL} = I_{rL} \quad (19)$$

Where V_{iL} and V_{rL} are the terminal forward travelling voltage and terminal backward travelling voltage, respectively.

From (17), it is shown that terminal reflection coefficient $\Gamma_L = -1$,which implies amplitude of forward travelling voltage wave at the terminal equals with that of backward travelling voltage wave while phase of those are 180-degree reversed. These two travelling voltage waves that add together leads to zero voltage at the terminal of the feeder, which is consistent with Fig.4 short-circuit waveform. On the contrary, both amplitude and phase of forward travelling current wave are the same as those of backward travelling current wave at the terminal. Moreover, from (13) (14) (18) and (19) amplitude of the voltage and current along the feeder can be expressed as:

$$|V_k(z)| = |V_{iL}(e^{j\beta z} - e^{-j\beta z})| = 2|V_{iL}||sin\beta z| = 2|A_1||sin\beta z| \quad (20)$$

$$|I_k(z)| = |I_{iL}(e^{j\beta z} + e^{-j\beta z})| = 2|I_{iL}||cos\beta z| = 2\frac{|A_1|}{Z_L}|cos\beta z| \quad (21)$$

Where harmonic peak voltage occurs at the $\frac{\lambda}{4}$ distance from terminal that is in agreement with Fig.4(a)(b)(c)(d) short circuit waveform as well. By further looking at the (20) and (21), amplitude of voltage and current depends on $|A_1|$ and Z_L where A_1 is expressed in (6). Therefore, if the length (l) of the feeder, distributed parameters (L and C), and terminal impedance (in this case $Z_L = 0$) are fixed, the amplitude only relies on harmonic frequency. So, the relationship between harmonic amplitude and harmonic frequency is further explored. From Fig.6 it is seen that at around 9th harmonic, the maximum harmonic voltage greatly amplified, at 3rd, 5th and 7th harmonic frequencies, the harmonic voltage amplification is not severe, which correspond to Fig.4 as well.

B. Open-circuit case

The terminal is open-circuited ($Z_L = \infty$), which means current amplitude at the terminal is zero. Therefore, substituting z=0 into (13) and (14) result in the following expression:

$$I_k(0) = \frac{1}{Z_0}(A_1 - A_2) = I_{iL} + I_{rL} = 0 \Rightarrow I_{iL} = -I_{rL} \quad (22)$$

$$V_L(0) = A_1 + A_2 = V_{iL} + V_{rL} = 2V_{iL} \Rightarrow V_{iL} = V_{rL} \quad (23)$$

By correlating (17) with (22), it is shown that $\Gamma_L = 1$, both amplitude and phase of forward voltage wave are the same as those of backward voltage wave, which indicates voltage amplitude at the terminal is twice that of forward travelling voltage as is shown in Fig.3(a)(b)(c) open-circuit waveform. Meanwhile, from (7)-(8) and (14)-(15) amplitude of the voltage and current along the feeder can be expressed in (24) and (25):
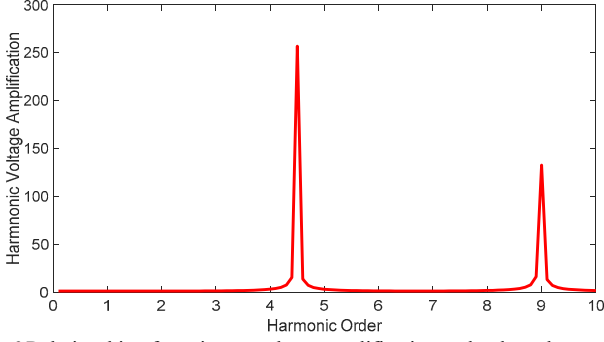
Fig.6 Relationship of maximum voltage amplification and voltage harmonics at short circuit case

$$|V_k(z)| = 2|V_{i2}||cos\beta z| = 2|A_1||cos\beta z| \qquad (24)$$

$$|I_k(z)| = 2|I_{i2}||sin\beta z| = 2\frac{|A_1|}{Z_L}|sin\beta z| \qquad (25)$$

Where harmonic peak voltage occurs at the terminal that conforms to Fig.3 open circuit waveform. Meanwhile, amplitude of voltage and current are contingent on length of feeder, terminal impedance, characteristic impedance and frequency, as has been discussed in short-circuit case. Moreover, the relationship between the maximum harmonic voltage and harmonic order is further explored, it is shown from Fig.7 that at 7th harmonic, voltage is extremely amplified to over 5 times of PCC fifth harmonic. 3rd, 5th and 9th maximum harmonic amplification does not exceed 2, which correspond to Fig.4.
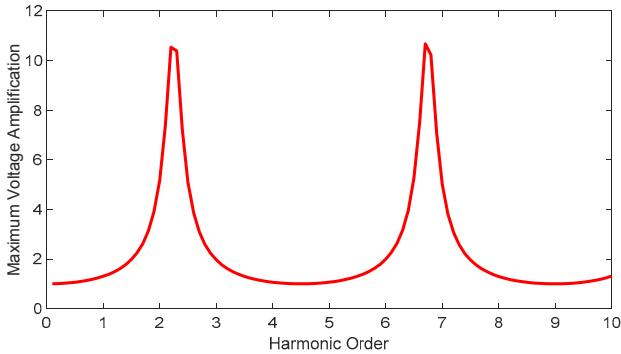

Fig.7 Relationship of maximum voltage amplification and voltage harmonics at open-circuit case

C. Pure Inductance Case

A pure inductance ($Z_L = jX_L$) is connected at the terminal, thus the terminal reflection coefficient is express as:

$$\Gamma_L = \frac{Z_L-Z_0}{Z_L+Z_0} = \frac{jX_L-Z_0}{jX_L+Z_0} = |\Gamma_L|e^{j\varphi_L} \qquad (26)$$

Where $|\Gamma_L| = 1$, $\varphi_L = \arctan(\frac{2X_LZ_0}{X_L^2-Z_0^2})$, its maximum amplitude of voltage and current lies between 0 and $\frac{\lambda}{4}$ of selected harmonic voltage. In addition, From Fig.8 it is observed that the dominant

concerned harmonic (3rd, 5th, 7th and 9th) amplification is low as well.

From above analysis, it is observed in all these three cases that terminal voltage coefficient $|\Gamma_L| = 1$ indicates the harmonic propagation as the standing waveform, where all the harmonic energy stored in the feeder, leading to no energy transmission. This is also the reason why "whack-a-mole" phenomenon occurs along the feeder.
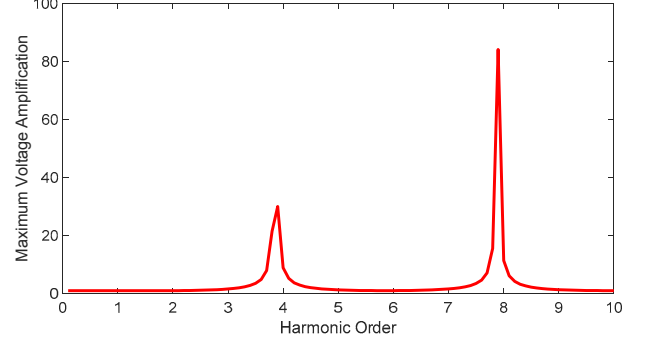

Fig.8 Relationship of maximum voltage amplification and voltage harmonics at pure inductance case

IV. HARMONIC DAMPING PERFORMANCE

It has been elaborated that when VCM-based DG unit with LC filter or CCM-based DG unit with LCL filter operates with R-APF control strategy, the DG unit at the selected frequency can be tuned as a pure resistance[12]. In contrast, VCM-based DG unit with LCL filter and R-APF control can only be tuned as complex impedance (*R-L*) without LCL filter grid side inductance compensation. Therefore, harmonic voltage amplification along the feeder need to be investigated when the equivalent complex impedance or resistance is connected at the feeder. Fig.9 illustrate the 3rd, 5th,7th and 9th harmonic voltage amplification along the 10km feeder when various types of virtual impedance embedded in DG unit control diagram such as $Z_L = R_L = Z_0, Z_L = R_L < Z_0 \ Z_L = R_L > Z_0, Z_L = R_L + jX_L$.

A. Terminal is connected to resistance

The terminal is interfaced to virtual resistance whose value is equivalent to characteristic impedance ($Z_L = R_L = Z_0$), based on (9) and (17) $\Gamma_L = 0, A_2 = 0$, thus, voltage and current along the feeder is expressed as (27) and (28), which reveals the harmonic energy is fully absorbed by the terminal impedance, so there does not exist the backward travelling wave without which amplitude of voltage and current are constant along the feeder as is shown in Fig.9 $Z_L = Z_0$ waveform. It is noteworthy that this conclusion also corresponds to the surge impedance loading condition of transmission line [1].

$$V_k(x) = A_1e^{-j\beta x} \qquad (27)$$

$$I_k(x) = \frac{A_1}{Z_L}e^{-j\beta x} \qquad (28)$$

In addition, either $Z_L = R_L > Z_0$ or $Z_L = R_L < Z_0$ leads to $|\Gamma_L| < 1$, the difference lies in that in the situation of $Z_L = R_L > Z_0$ maximum amplitude of voltage is at the terminal of the

feeder, on the contrary, when $Z_L = R_L < Z_0$, the minimum amplitude of voltage is at the terminal of the feeder, as is shown in Fig.9.

B. Terminal is connected to complex impedance

The terminal is interfaced to a complex impedance $Z_L = R_L + jX_L$, the reflection coefficient is at the terminal calculated as:

$$\Gamma_L = \Gamma_{L1} + \Gamma_{L2} = \frac{Z_L - Z_0}{Z_L + Z_0} = \frac{R + jX_L - Z_0}{R + jX_L + Z_0}$$

$$\Rightarrow |\Gamma_L| = \sqrt{\frac{(R_L - Z_0)^2 + X_L^2}{(R_L + Z_0)^2 + X_L^2}} \qquad (29)$$

Where the reflection coefficient $|\Gamma_L| < 1$, which implies parts of forwarding travelling wave is absorbed by impedance. Amplitude of waveform is expressed in (30)-(31), showing the maximum voltage amplification and minimum voltage amplification have the following relationship: $|V_{i2}| < |V_{max}| < 2|V_{i2}|$, $0 < |V_{min}| < |V_{i2}|$.

$$|V(z)| = |V_{i2}|\sqrt{1 + |\Gamma_L|^2 + 2|\Gamma_L|\cos(2\beta x - \varphi_L)} \qquad (30)$$

$$|I(z)| = |I_{i2}|\sqrt{1 + |\Gamma_L|^2 - 2|\Gamma_L|\cos(2\beta x - \varphi_L)} \qquad (31)$$

V. DG'S CONTROL STRATEGY FOR HARMONIC PROPAGATION DAMPING

It is demonstrated that the grid side inductor L_2 can affect the harmonic voltage damping[12] when DG with LCL filter works at VCM mode. In order to reduce the impact of LCL filter grid-side inductor, a modified control algorithm needs to be investigated. An intuitive to reduce the impact of grid side inductor of LCL filter is to subtract a negative virtual inductor as the compensation as is shown (24)

$$V_{ref} = V_{vef1} - V_{AD} - V_{comp}$$

$$= V_{vef1} - R_v \cdot H_{BPF}(s)I_g - s(-L_2) \cdot H_{BPF}(s)I_g \qquad (32)$$

Where V_{verf1} is the fundamental voltage reference derived from droop control. V_{AD} is harmonic voltage reference for virtual impedance shaping, V_{comp} is the voltage drop on negative inductance, $H_{BPF}(s)$ is the band-pass filter transfer function. However, the virtual inductor compensation involves a derivative term, which amplifies the noise of the system. To overcome this drawback, derivative term can be replaced by selected frequencies. So, V_{comp} is expressed as:

$$V_{comp} = jw_5(-L_2)H_{BPF5}(s) + jw_7(-L_2)H_{BPF7}(s) + jw_9(-L_2)H_{BPF9}(s) \qquad (33)$$

The control diagram of DG unit with inductor voltage compensation is shown in Fig.10. As is illustrated, single DG with LCL filter is connected to long feeder. $P - f$ and $Q - E$ droop control is implemented to generate the fundamental voltage reference V_{vef1}. Besides, four band-pass filters are implemented to extract the selected harmonic current. Moreover, virtual impedances at the selected frequency are separately designed to optimize the harmonic mitigation along the feeder.
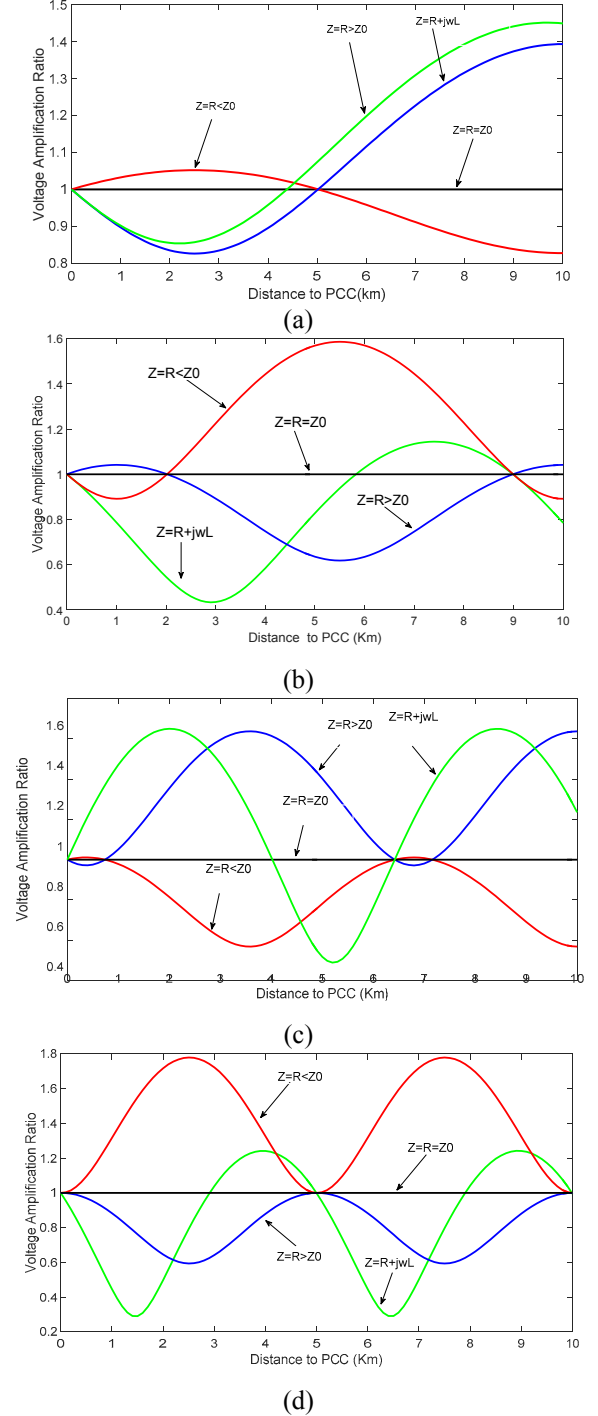
(a)

(b)

(c)

(d)

Fig.9.Harmonic voltage amplification ratio when 3rd(a), 5th(b), 7th(c), 9th (d) harmonic voltage source is interfaced to damping impedance through long feeder
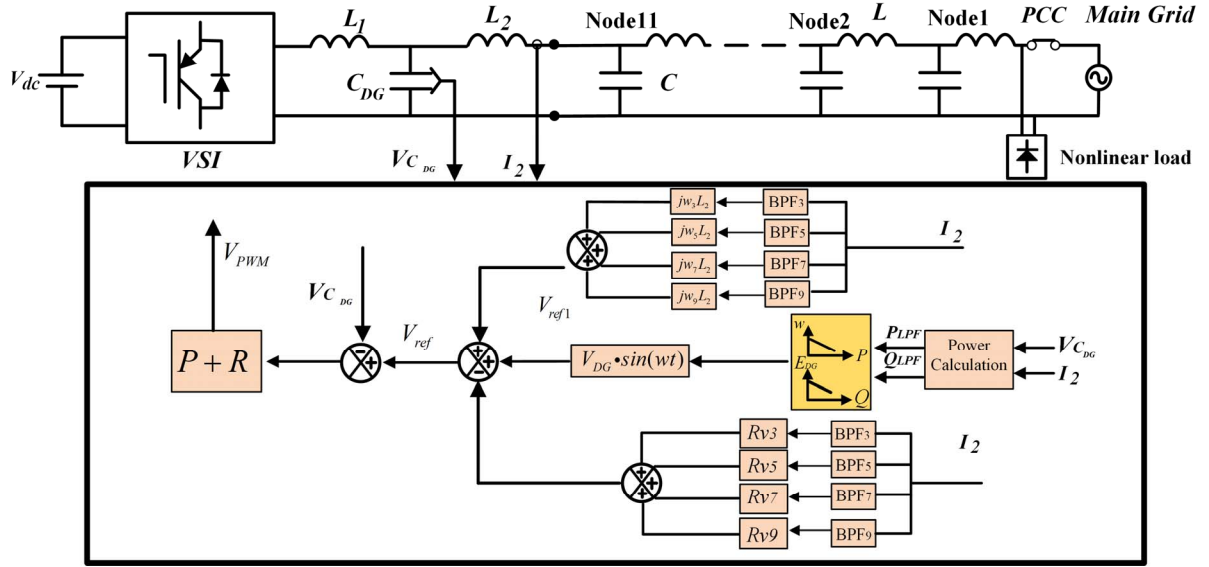
Fig.10. Control diagram of proposed method

Virtual impedance selection of DG unit takes a crucial role in harmonic damping along the feeder. Ideally, harmonic voltage will not propagate along the feeder if the virtual impedance is selected to equal characteristic impedance [4]. However, in reality, impedance matching can hardly be achieved due to inherent damping of parasitic resistor and uneven feeder Inductance and capacitance. Plotting of the harmonic voltage amplification of various value of terminal impedance is an effective way for selection of virtual impedance. As is shown in Fig.9 (a), if the virtual impedance for the third harmonic is less than characteristic impedance (In this plot, Z = 7Ω), harmonic is damped out from node 5 to end of the feeder, On the contrary, it slightly amplified from PCC to Node 4. For the same reason, As is shown in Fig.9 (b) (c) and (d), harmonic mitigation can achieve best effect when the 5th and 9th virtual impedance is greater than characteristic impedance while 7th virtual impedance is less than characteristic impedance.

TABLE II.   DG CONTROL PARAMETER

Parameter	Value
Droop Coefficient	$D_p = 1/250$ $D_Q = 1/250$
Sampling frequency	10kHz
LCL filter	$L_1 = 2mH, L_2 = 3.5mH, C_{DG} = 20uF$
Virtual Impedance R_V	$R_{V5} = 7Ω$ $R_{V5} = 15Ω$ $R_{V7} = 7Ω$ $R_{V9} = 15Ω$

VI. CASE STUDY RESULTS

Simulation results are provided to verify the proposed control strategies. The simulated system parameters are shown in Table 2. Single DG with LCL filter is tested in Matlab/Simulink, PCC voltage is assumed stiff and has 3% distortion at 3th, 5th, 7th,9th harmonic frequency and the total THD is 6.01%, as is shown in Table 3. When VCM without virtual impedance damping and negative inductor compensation

is adopted in the DG unit, PCC voltage, node1,3,5,7, and DG capacitor voltage waveforms are shown in Fig.11, the harmonic distortion at each frequency and THD of each nodes are presented in the TABLE 3. As is seen from Fig.11, DG capacitor voltage is almost sinusoidal and harmonic free but other nodes of the feeder is highly polluted by the harmonics.
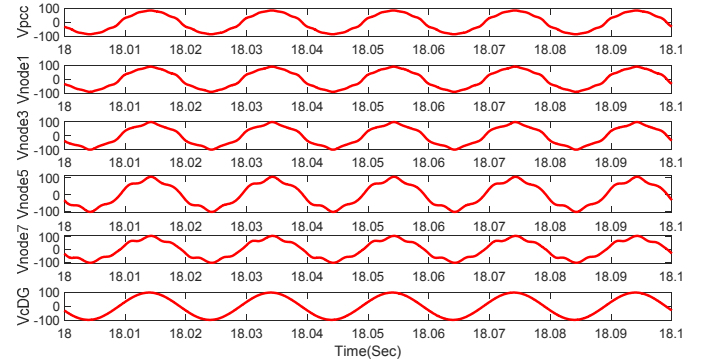

Fig.11 Voltage distortion along the feeder without harmonic damping

TABLE III.   HARMONIC SPECTRUM WITH CONVENTIONAL CONTROL

	3th	5th	7th	9th	THD
PCC	3%	3%	3%	3%	6.01%
Node1	3%	5.58%	2.06%	3.17%	7.39%
Node3	2.84%	9.68%	0.268%	2.1%	10.32%
Node5	2.51%	11.78%	2.16%	0.19%	12.44%
Node7	2.05%	11.62%	3.26%%	2.17%	12.44%
$V_C DG$	0.06%	0.11%	0.01%	0.02%	0.4%

When the proposed control strategy is applied to DG unit, harmonic drops on the grid-side inductor of DG is compensated, meanwhile, to optimize the THD on each node, virtual impedances at the selected frequency are separately designed based on aforementioned discussion. A corresponding harmonic spectrum group is shown in Fig.9 and Table 4 where harmonic at each node is greatly mitigated compared to the Table 3.

TABLE I.   HARMONIC SPECTRUM WITH PROPOSAL CONTROL

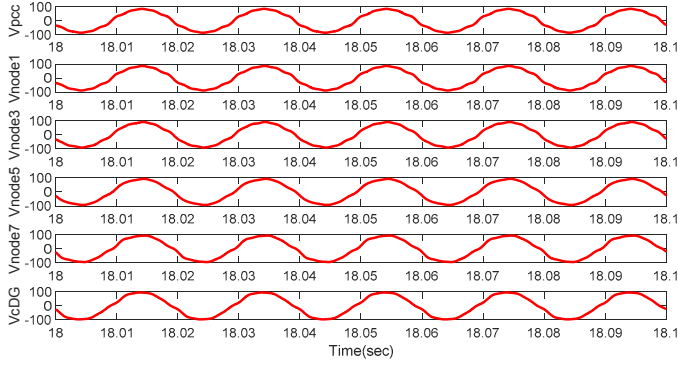|	3th	5th	7th	9th	THD
PCC	3%	3%	3%	3%	6.01%
Node1	3.02%	2.68%	2.5%	3.32%	5.81%
Node3	2.9%	2.83%	1.44%	2.68%	5.08%
Node5	2.65%	3.52%	1.65%	1.16%	4.86%
Node7	2.28%	4.01%	2.5%	2.04%	5.65%
$V_C DG$	1.05%	3.25%	1.7%	1.63%	4.17%

Fig.12 Voltage distortion along the feeder with proposed control

VII. CONCLUSION

In this paper, harmonic resonance and propagation of distribution line is first investigated. In order to have a depth understanding of the phenomenon of "whack-a-mole", theoretical analysis is conducted by placing the original point of coordinate to the end of the feeder. It is shown that standing waveform of harmonic lead to the propagation along the distribution feeder. In order to alleviate the harmonic propagation, the performance of various damping impedance is examined as well. Finally, this paper proposed one method to mitigate the harmonic propagation and influence of grid-side inductor. Simulation are conducted to show the effectiveness of the proposed method.

REFERENCES

[1] M. F. M. R.C. Dugan, and H.W, "Electrical Power Systems Quality," *New York: McGraw-Hill, 1996*.

[2] H. Akagi, Y. Kanazawa, and A. Nabae, "Instantaneous Reactive Power Compensators Comprising Switching Devices without Energy Storage Components," *Industry Applications, IEEE Transactions on,* vol. IA-20, pp. 625-630, 1984.

[3] T. L. Lee and S. H. Hu, "Discrete Frequency-Tuning Active Filter to Suppress Harmonic Resonances of Closed-Loop Distribution Power Systems," *IEEE Transactions on Power Electronics,* vol. 26, pp. 137-148, 2011.

[4] K. Wada, H. Fujita, and H. Akagi, "Considerations of a shunt active filter based on voltage detection for installation on a long distribution feeder," *Industry Applications, IEEE Transactions on,* vol. 38, pp. 1123-1130, 2002.

[5] L. Tzung-Lin, L. Jian-Cheng, and C. Po-Tai, "Discrete Frequency Tuning Active Filter for Power System Harmonics," *Power Electronics, IEEE Transactions on,* vol. 24, pp. 1209-1217, 2009.

[6] L. Tzung-Lin, C. Po-Tai, H. Akagi, and H. Fujita, "A Dynamic Tuning Method for Distributed Active Filter Systems," *Industry Applications, IEEE Transactions on,* vol. 44, pp. 612-623, 2008.

[7] X. Sun, R. Han, H. Shen, B. Wang, Z. Lu, and Z. Chen, "A Double-Resistive Active Power Filter System to Attenuate Harmonic Voltages of a Radial Power Distribution Feeder," *IEEE Transactions on Power Electronics,* vol. 31, pp. 6203-6216, 2016.

[8] H. Jinwei, L. Yun Wei, D. Bosnjak, and B. Harris, "Investigation and Active Damping of Multiple Resonances in a Parallel-Inverter-Based Microgrid," *Power Electronics, IEEE Transactions on,* vol. 28, pp. 234-246, 2013.

[9] H. Jinwei, L. Yun Wei, F. Blaabjerg, and W. Xiongfei, "Active Harmonic Filtering Using Current-Controlled, Grid-Connected DG Units With Closed-Loop Power Control," *Power Electronics, IEEE Transactions on,* vol. 29, pp. 642-653, 2014.

[10] H. Jinwei, L. Yun Wei, and M. S. Munir, "A Flexible Harmonic Control Approach Through Voltage-Controlled DG and Grid Interfacing Converters," *Industrial Electronics, IEEE Transactions on,* vol. 59, pp. 444-455, 2012.

[11] D. Pozar, *Microwave Engineering* vol. 752: Wiley, 2011.

[12] H. Jinwei, L. Yun Wei, W. Ruiqi, and Z. Chenghui, "Analysis and Mitigation of Resonance Propagation in Grid-Connected and Islanding Microgrids," *Energy Conversion, IEEE Transactions on,* vol. 30, pp. 70-81, 2015.